COMPUTATION OF FLOW OVER A SPHERICALLY BLUNTED CONE FOR VARIOUS SHOCK LAYER AND SURFACE BLOWING CONDITIONS

A. V. Bureev and V. I. Zinchenko

UDC 533.6.011.536.24

The authors examine axisymmetric supersonic air flow over a spherically blunted cone at Reynolds numbers where various flow regimes exist in the shock layer. The influence of surface blowing on the characteristics of the laminar and turbulent viscous shock layer was analyzed in [1, 2]. This paper addresses the influence of blowing intensity and the distribution laws of the blown gas along the spherical blunting generator on the characteristics of heat and mass transfer and compares the results with the experimental data of [3].

1. In the natural coordinate system (s, n) the system of equations of the viscous shock layer for mean quantities, using the dimensionless variables introduced in [4], has the form

$$\frac{\partial}{\partial s}(\rho u r) + \frac{\partial}{\partial n}(\rho v r h_1) = 0; \tag{1.1}$$

$$\rho\left(\frac{u}{h_1}\frac{\partial u}{\partial s} + v\frac{\partial u}{\partial n} + \frac{kuv}{h_1}\right) = -\frac{1}{h_1}\frac{\partial p}{\partial s} + \varepsilon^2\frac{\partial}{\partial n}\left[\mu_\Sigma\left(\frac{\partial u}{\partial n} - \frac{ku}{h_1}\right)\right] + \varepsilon^2\mu_\Sigma\left(\frac{2k}{h_1} + \frac{\cos\alpha}{r}\right)\left(\frac{\partial u}{\partial n} - \frac{ku}{h_1}\right); \tag{1.2}$$

$$\rho\left(\frac{u}{h_1}\frac{\partial v}{\partial s} + v\frac{\partial v}{\partial n} - \frac{ku^2}{h_1}\right) = -\frac{\partial p}{\partial n}; \tag{1.3}$$

$$\rho\left(\frac{u}{h_1}\frac{\partial H}{\partial s} + v\frac{\partial H}{\partial n}\right) - v\left(\frac{\partial p}{\partial n} - \frac{k\rho u^2}{h_1}\right) = \varepsilon^2\frac{\partial}{\partial n}\left[\frac{\mu_\Sigma}{\mathrm{Pr}_\Sigma}\frac{\partial H}{\partial n} + \frac{\mu_\Sigma}{\mathrm{Pr}_\Sigma}(\mathrm{Pr}_\Sigma - 1)u\frac{\partial u}{\partial n} - \mu_\Sigma\frac{ku^2}{h_1}\right] + \varepsilon^2\left(\frac{k}{h_1} + \frac{\cos\alpha}{r}\right)\left[\frac{\mu_\Sigma}{\mathrm{Pr}_\Sigma}\frac{\partial H}{\partial n} + \frac{\mu_\Sigma}{\mathrm{Pr}_\Sigma}(\mathrm{Pr}_\Sigma - 1)u\frac{\partial u}{\partial n} - \mu_\Sigma\frac{ku^2}{h_1}\right]; \tag{1.4}$$

$$p = \rho h(\gamma - 1)/\gamma. \tag{1.5}$$

The boundary conditions at the shock ($n = n_s$) for the range of Reynolds number considered is written as the ordinary Rankine–Hugoniot relations:

$$u_s = \cos\sigma\cos\beta_s + \frac{1}{\rho_s}\sin\sigma\sin\beta_s,$$

$$v_s = u_s\,\mathrm{tg}\,\beta_s - \frac{1}{\rho_s}\frac{\sin\sigma}{\cos\beta_s}, \quad p_s = \frac{1}{\gamma M_\infty^2} + \left(1 - \frac{1}{\rho_s}\right)\sin^2\sigma, \tag{1.6}$$

$$H_s = H_\infty, \quad \frac{1}{\rho_s} = \frac{\gamma - 1}{\gamma + 1} + \frac{2}{(\gamma + 1)M_\infty^2\sin^2\sigma}.$$

On the body ($n = 0$) for blown gas of the same composition as the incident stream gas we have

$$u = 0, \ (\rho v) = (\rho v)_w(s), \ h = h_w. \tag{1.7}$$

The conditions on the axis of symmetry ($s = 0$) are:

$$u = 0, \ \partial v/\partial s = \partial p/\partial s = \partial H/\partial s = 0. \tag{1.8}$$

The shock slope angle σ is associated with the standoff distance n_s by the relation $dn_s/ds = h_{1s}\tan\beta_s$, $\beta_s = \sigma - \alpha$.

In Eqs. (1.1)-(1.8) u and v are the components of the vectorial velocity, referenced to v_∞; p, ρ are the gas pressure and density, referenced to $\rho_\infty v_\infty^2$ and ρ_∞, respectively; $H = h + u^2/2$ is the enthalpy, referenced to v_∞^2; T is the temperature, referenced to the characteristic value $T_* = v_\infty^2/c_p$; μ is the coefficient of viscosity, referenced to its own characteristic value, $\mu_*(T_*)$; $h_1 = 1 + kn$, $r = r_w + n\cos\alpha$ are Lamé coefficients; $\varepsilon^2 = \mu_*/(\rho_\infty v_\infty R_N)$ is a dimensionless parameter, the inverse Reynolds number; $\mu_\Sigma = \mu + \Gamma\mu_t$; $\mathrm{Pr}_\Sigma = \mu_\Sigma\mathrm{Pr}\mathrm{Pr}_t/(\mu\mathrm{Pr}_t + \Gamma\mu_t\mathrm{Pr})$; the subscripts ∞, s, and w refer to the flow characteristics in the incident stream, behind

Tomsk. Translated from Zhurnal Prikladnoi Mekhaniki i Tekhnicheskoi Fiziki, No. 2, pp. 100-106, March-April, 1991. Original article submitted October 20, 1989.

 0021-8944/91/3202-0236$12.50

the shock wave, and on the body surface, respectively; t refers to quantities associated with turbulent transfer.

We find the coefficient of molecular viscosity from the Sutherland formula $\mu = \left(\frac{1+C}{T+C}\right) T^{3/2}$, $C = \frac{110.4}{(\gamma-1)\,M_\infty^2 T_{\infty p}}$ ($T_{\infty p}$ is the dimensionless temperature). We determine the coefficient of turbulent viscosity μ_t using the two-layer model of [5]. For the dimensionless variables used we can write for the wall region

$$\mu_t = \frac{0{,}16\rho n^2}{\varepsilon^2}\left[1 - \exp\left(-\frac{n}{A}\right)\right]^2 \frac{\partial u}{\partial n},$$

$$A = \varepsilon^2 \frac{26\mu}{\rho v_*}\left[\frac{\bar{P}}{\bar{v}_w}\left(1 - \exp\left(11{,}8\bar{v}_w\right)\right) + \exp\left(11{,}8\bar{v}_w\right)\right]^{-1/2},$$

$$\bar{v}_w = \frac{v_w}{v_*},\quad v_* = \varepsilon\sqrt{\frac{\tau_w}{\rho}},\quad \bar{P} = -\frac{\varepsilon^2\mu}{\rho\rho_w v_*^3}\frac{\partial p_e}{\partial s},\quad \tau_w = \mu_w \frac{\partial u}{\partial n}\Big|_w.$$

In the outer region we have

$$\mu_t = \frac{0{,}0168}{\varepsilon^2}\rho\left[1 + 5{,}5\left(\frac{n}{n_e}\right)^6\right]^{-1}\int_0^{n_e}(u_e - u)\,dn.$$

Here and below the subscript e denotes the characteristics at the outer edge of the boundary layer in the shock layer; the values n_e and u_e vary due to variation of the shock layer boundary, and we evaluate their influence on the flow quantities at the body surface.

We computed the transition flow region using the formulas of [6]. For flow over a spherically blunted body the intermittence coefficient Γ can be written in the form

$$\Gamma = 1 - \exp\left[-\frac{\Phi \sin s}{\frac{1}{R_N}\frac{du_e}{ds}\Big|_{s=0}}\ln\left(\frac{\operatorname{tg}\frac{s}{2}}{\operatorname{tg}\frac{s_p}{2}}\right)\ln\frac{s}{s_p}\right],$$

$$\Phi = \frac{3n_e^3}{\varepsilon^4\left(B\frac{\mu_e}{\rho_e}\right)^2}\mathrm{Re}_p^{-1{,}34},\quad B = 60 + 4{,}68M_p^{1{,}92},$$

where $\mathrm{Re}_p = \frac{1}{\varepsilon^2}\frac{\rho_e u_e s_p}{\mu_e}$, $M_p = \left(\frac{u_e}{a_e}\right)_{s\,=\,s_p}$ are the Reynolds and Mach numbers computed at the point where the laminar boundary layer loses stability. The coordinate of this point s_p, representing the start of the flow transition region, was either defined experimentally or was computed from the critical Reynolds number

$$\mathrm{Re}^{**} = \frac{1}{\varepsilon^2}\frac{\rho_e u_e \delta^{**}}{\mu_e} = 200,\quad \delta^{**} = \int_0^{n_e}\frac{\rho u}{\rho_e u_e}\left(1 - \frac{u}{u_e}\right)dn.$$

In the laminar flow regime region $\Gamma = 0$, and in the region of turbulent flow $\Gamma = 1$.

2. Methods based on global iterations of the shock wave shape [4, 7] are efficient methods of solving the system of equations of the viscous shock layer. To compute the system of equations (1.1)-(1.5) we used the following transformation of the independent variables [7]:

$$\xi = s,\quad \eta = \frac{1}{\Delta}\int_0^n \rho\left(\frac{r}{r_w}\right)dn,\quad \Delta = \int_0^{n_s}\rho\left(\frac{r}{r_w}\right)dn.$$

Using the global iteration method, for which the computing technique has been described in detail in [8], we numerically integrated the original boundary problem over a wide range of variation of Reynolds and Mach number. To stabilize the iteration process in the ongoing global iteration we used the slope of the curvature parameter at the point of discontinuity in the curvature of the sphere-cone generator. Difference schemes for systems of equations of parabolic and hyperbolic type were obtained using the interaction-interpolation method of [9]. For the turbulent flow regime in the shock layer we developed combined difference

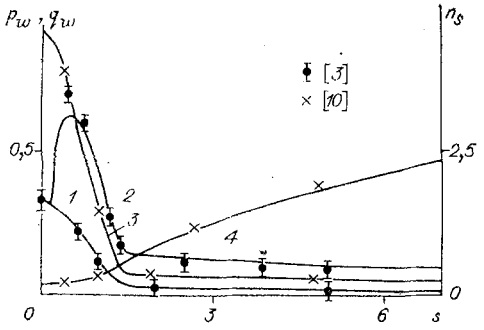

Fig. 1

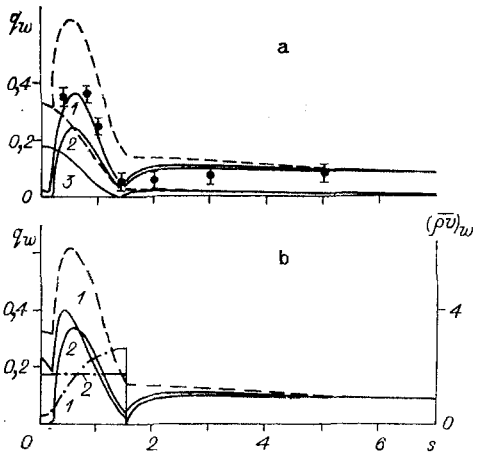

Fig. 2

schemes to ensure smoothing of the described characteristics in the laminar sublayer region and the turbulent core, and taking account of the nature of the variation of the turbulent viscosity across the shock layer. This increased the rate of convergence of the iterative process and allowed computation to $Re_\infty = 10^8$-10^9 for various flow rates of blown gas from the wetted body surface. For a turbulent flow regime across the shock layer we used a variable step size to achieve the required number of computing points in the laminar sublayer. As a test we used computations according to the boundary layer model and the Euler model.

3. Figures 1 and 2 show results computed for flow over a spherically blunted cone of semivertex angle 5°, for governing parameters simulating the experimentally measured thermal characteristics with surface blowing in a wind tunnel [3]. The test conditions were $M_\infty = 5$. stagnation temperature $T_{e0} = 525$ K, $T_w = 288$ K, model radius $R_N = 0.0508$ m, stagnation pressure $p_{e0} = 0.625 \cdot 10^5$ and $3.125 \cdot 10^5$ N/m^2 for the laminar and turbulent flow regimes, respectively.

Figure 1 shows curves of distribution of the dimensionless heat flux $q_w = \left(\frac{\mu}{\mathrm{Pr}}\frac{\partial H}{\partial n}\right)_w \frac{\sqrt{\mathrm{Re}}}{\rho_{e0} v_m h_{e0}}$ for laminar and turbulent flow regimes in the shock layer (curves 1, 2), the surface pressure p_w, and the shock standoff distance n_s (curves 3, 4), with no surface gas blowing. In the expression for q_w the quantity $\left(\frac{\mu}{\mathrm{Pr}}\frac{\partial H}{\partial n}\right)_w$ is the dimensional heat flux, and $\mathrm{Re} = \frac{\rho_{e0} v_m R_N}{\mu_{e0}}$ ($v_m = \sqrt{2h_{e0}}$) is connected with ε^2 as follows: $\varepsilon^2 = \frac{\rho_{e0}}{\rho_\infty}\frac{v_m}{v_\infty}\left(\frac{\mu_{e0}}{\mu_*}\mathrm{Re}\right)^{-1}$. For the conditions assumed $\mathrm{Re} = 7.74 \cdot 10^5$ and $3.87 \cdot 10^6$. Here we also show the experimentally measured heat flux from [3] and the theoretical characteristics from the tables of [10]. With the dimensionless quantities assumed the heat fluxes in the section where the laminar flow regime holds coincide, but in the developed turbulence regime q_w increases appreciably and the maximum heat flux is reached in the vicinity of the sonic line. The surface pressure and the position of the shock wave coincide for the values of Re examined.

The influence of gas blowing from the spherically blunted surface at constant mass flow levels $(\rho v)_w$ on the heat flux is shown in Fig. 2a, where curves 1 and 2 correspond to turbulent flow ($\mathrm{Re} = 3.87 \cdot 10^6$) with $(\overline{\rho v})_w = 1.52$; and for curve 3 (the dimensionless mass flow $(\overline{\rho v})_w$ is associated with the dimension: $(\overline{\rho v})_w = \frac{(\rho v)_w \sqrt{\mathrm{Re}}}{\rho_{e0} v_m}$). Curve 3 was obtained for laminar flow with $(\overline{\rho v})_w = 0.5$. The broken lines of Fig. 2 are taken from Fig. 1 with $(\overline{\rho v})_w = 0$, and by comparing the corresponding curves we can analyze the attenuation of heat flux in the thermal curtain zone on the conical part of the surface. The symbols [for $(\overline{\rho v})_w = 1.52$] indicate the experimental data, which agree quite saisfactorily with the computed values on the spherical part of the body in the turbulent flow region. On the conical surface the computed values behind the conjugate point with the spherical nose for $s < 5.0$ lie markedly above the experimental data, which was also noted in [3], the reason for the lack of agreement perhaps being the unsteady nature of the heat transfer processes occurring in the conduct of the experiment.

For the computed Re and the above flow rates of blown gas (see Fig. 2) we observe a strong decrease of heat flux, but here the surface pressure and the standoff distance remain practically unchanged. Thus, for large Re in the various flow regimes in the shock layer we

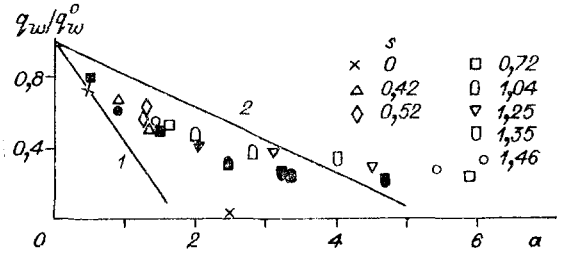

Fig. 3

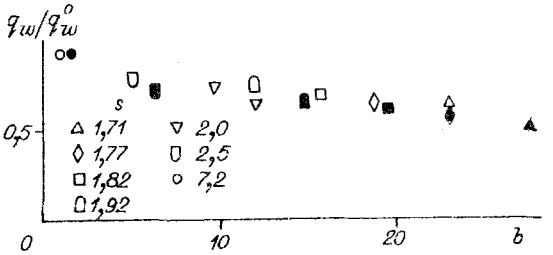

Fig. 4

find a range of blown gas flow rate to achieve the required decrease of heat flux to the body, and therefore the allowance shell temperature conditions while retaining the aerodynamic characteristics.

It is of interest to evaluate the influence of the blown gas distribution law on the heat flux to the spherical porous shell and the conical surface. In Fig. 2b the curves 2 show the heat flux $q_w(s)$ for $(\overline{\rho v})_w(s)$ = const = 1.785 (the dot–dash line 2), and the curves 1 were obtained for the mass flow rate distribution shown by the dot–dash line 1. Here the total mass of coolant gas $2\pi R_N^2 \int_0^{s_1} (\rho v)_w \sin s ds$ is the same for both cases, but the mass flow rate law was obtained by assigning the pressure p_k in the cavity of the porous spherical shell. Using the equation of motion for a thin porous shell in steady state in the form of the Darcy law, allowing for the quadratic term

$$\partial p / \partial n = A\mu v + B\rho v^2 \varphi \tag{3.1}$$

and the mass conservation law

$$(\rho v \varphi) = (\rho v)_w, \tag{3.2}$$

it is straightforward, after integrating Eq. (3.1) and using the equation of state P = ρRT/M, to write the expression

$$(\rho v)_w = \left[-A\mu + \sqrt{(A\mu)^2 + \frac{2B\varphi}{TL\frac{R}{M}} \left(p_k^2 - p_w^2\right)} \right] \frac{1}{2B}. \tag{3.3}$$

For typical values of the structural characteristics of materials A and B, porosity φ [11] and a given shell thickness L, one can easily determine the blown gas flow rate rate $(\rho v)_w(s)$.

As one might expect, for the flow rate law determined for the frontal part of the spherical shell in the laminar flow region, and for part of the turbulent flow region the heat fluxes q_w exceed the corresponding values obtained for a constant flow rate, while on the lateral surfaces they are reduced compared with curve 2. On the whole the length of the thermal curtain is determined by the total mass of cold blown gas, and for the laws of $(\overline{\rho v})_w \times (s)$ considered it depends weakly on the nature of the blowing distribution along the generator.

For a porous spherical shell Fig. 3 shows the results of reducing the solution of $q_w(s)/q_w^0(s)$ as a function of the dimensionless parameter $a = (\rho v)_w(H_{e0} - H_w)/q_w^0$ at various points along the contour. Here $q_w^0(s)$ is the heat flux with no blowing; the open points show the computed data, and the closed points are the experimental values [3]. Curve 1 was obtained from a formula of [12] for the vicinity of the forward stagnation point and corresponds to laminar flow, and curve 2 corresponds to a formula of [13] for turbulent flow on a plate. It can be seen that in the region of developed turbulence on the sphere the results agree satisfactorily with experimental data and can be used to evaluate the influence of blowing on the flux. In processing the computations we used different laws for $(\rho v)_w(s)$ (constant flow rate), and also dependence (3.3).

Figure 4 shows the reduced results of solving on the conical part of the body in the thermal curtain zone for turbulent flow. As was done in [14], as a blowing parameter we took the ratio of the total mass of blown gas to the product of the heat transfer coefficient at the section considered with no blowing to the surface area Π(s) from the line where the blowing ends to the section considered $b = 2\pi R_N^2 \int_0^{s_1} (\rho v)_w \sin s ds (H_{e0} - h_w)/(q_w^0(s)\,\Pi(s))$. The open and closed

points show the constant flow rate case and Eq. (3.3), respectively. Processing of the experimental data of [3] also gives values close to the theory. We note that the results obtained lie above the data of [14], which is evidently due to the difference of geometry of the wetted bodies and to the unsteady nature of the heat transfer process in an experiment conducted on thermally nonconducting materials in the zone behind the blowing section. For these conditions of the isothermal surface from the data reduction we can evaluate the heat flux to the conical surface as a function of the governing parameters of the problem.

LITERATURE CITED

1. A. Kumar, S. N. Tiwari, and R. A. Graves, "Laminar and turbulent flows over a spherically blunted cone with massive surface blowing," AIAA J., 17, No. 12 (1979).
2. J. N. Moss, A. Simmonds, and E. C. Anderson, "Turbulent radiating shock layers with coupled ablation injection," AIAA J., 19, No. 2 (1981).
3. R. H. Feldhuhm, "Heat transfer from a turbulent boundary layer on a porous hemisphere," AIAA Paper No. 119, New York (1976).
4. R. T. Davis, "Numerical solution of the hypersonic viscous shock layer equations," AIAA J., 8, No. 5 (1970).
5. T. Cebeci, "Behavior of turbulent flow near a porous wall with pressure gradient," AIAA J., 8, No. 12 (1970).
6. K. K. Chen and N. A. Tyson, "Extension of Emmons spot theory to flow on blunt bodies," AIAA J., 9, No. 5 (1971).
7. S. A. Vasil'evskii and G. A. Tirskii, "Some methods of numerical solution of the equations of the viscous shock layer," in: Aerodynamics of Hypersonic Flow with Blowing [in Russian], Izd. Mosk. Gos. Univ., Moscow (1979).
8. V. I. Zinchenko and S. I. Pyrkh, "Computation of the nonequilibrium viscous shock layer, accounting for coupled heat transfer," Izv. Akad. Nauk SSSR, Mekh. Zhidk. Gaza, No. 2 (1984).
9. A. M. Grishin, V. N. Bertsun, and V. I. Zinchenko, The Iterative–Interpolative Method and Its Applications [in Russian], Izd. Tomsk Gos. Univ., Tomsk (1981).
10. A. N. Lyubimov and V. V. Rusanov, Flow of a Gas over Blunt Bodies [in Russian], Part 1, Nauka, Moscow (1970).

DYNAMICS OF LOW-AMPLITUDE PULSE WAVES IN VAPOR–GAS–DROP SYSTEMS

D. A. Gubaidullin and A. I. Ivandaev

UDC 532.529:534.2

The propagation of weak monochromatic waves in vapor and gas suspensions, as well as in gas, vapor, and fluid drop mixtures, was treated in [1-8]. In the present paper we present results on propagation of low-amplitude pulse perturbations in single- and two-component gas–drop systems. An evolution wave-like equation, describing the propagation of linear perturbations in single-component suspensions in the prsence of phase transformations, is obtained and analyzed. Using the fast Fourier transform method, the evolution of a single pulse perturbation in a two-component vapor–gas–drop mixture is calculated. The evolution of interphase friction and phase transformation effects on the wave evolution process are analyzed.

The two-velocity and three-temperature continuum model [9] is used under conditions of acoustic homogeneity of the monodisperse mixture under consideration to investigate a variety of effects. We write down the linearized equations of planar one-dimensional motion in the presence of phase transitions. In a coordinate system in which the unperturbed mixture is at rest the conservation equations of mass, momentum, and energy of the phases are [8]

$$\frac{\partial \rho_1'}{\partial t} + \rho_{10}\frac{\partial v_1'}{\partial x} = -n_0 j_{V\Sigma}, \quad \frac{\partial \rho_V'}{\partial t} + \rho_{V0}\frac{\partial v_1'}{\partial x} = -n_0 j_{V\Sigma}, \quad \frac{\partial \rho_2'}{\partial t} + \rho_{20}\frac{\partial v_2'}{\partial x} = n_0 j_{\Sigma},$$

$$\rho_{10}\frac{\partial v_1'}{\partial t} + \frac{\partial p_1'}{\partial x} + n_0 f = 0, \quad \rho_{20}\frac{\partial v_2'}{\partial t} = n_0 f,$$

Kazan'. Tyumen'. Translated from Zhurnal Prikladnoi Mekhaniki i Tekhnicheskoi Fiziki, No. 2, pp. 106-113, March-April, 1991. Original article submitted February 21, 1989; revision submitted November 18, 1989.

0021-8944/91/3202-0240$12.50